Tellus (1993), 45A, 462–477
Printed in Belgium - all rights reserved

TELLUS
ISSN 0280-6495

Examination of the accuracy of a tangent linear model

By RONALD M. ERRICO*, TOMISLAVA VUKIĆEVIĆ, and KEVIN RAEDER, *National Center for Atmospheric Research*[1], *Boulder, Colorado 80307–3000, USA*

(Manuscript received 9 November 1992; in final form 23 April 1993)

ABSTRACT

The accuracy of a tangent linear version of a 3-dimensional mesoscale primitive equation model (the PSU/NCAR MM4) is investigated by comparing its results with those produced by identical perturbations introduced in nonlinear forecasts of the original model. Moist physical processes are not considered in this study. For perturbation magnitudes as large as typical current analysis errors, the perturbation tendencies are shown to be very accurately estimated by the tangent linear model (TLM), with greater relative error in a summer case than in a winter one. The evolutions of perturbations in forecasts out to 72 h are also accurately estimated, although the unperturbed lateral boundary conditions that act to sweep perturbations out of the domain are an artificial means of perturbation constraint. It is shown that for many cases it is sufficient to approximate a true TLM by using an infrequent update of the basic state, thereby reducing the amount of stored fields and input required by the TLM software. For perturbations not smaller than one-tenth the size of typical analysis errors, a 30-min update appears sufficient. The TLM accuracy is related to the accuracy of adjoint sensitivity calculations with regard to finite-amplitude perturbations. An example of an adjoint application is shown to have two-digit accuracy for a moderately sized perturbation. All these results indicate that our TLM and corresponding adjoint yield quantitatively accurate results for many important uses.

1. Introduction

A tangent linear model (TLM) describes the evolution of perturbations in a forecast model (Lacarra and Talagrand, 1988). It uses approximations that are linear with respect to perturbations of the model fields. It is called a tangent model because the linearization is around a time-evolving solution, and therefore, the coefficients of the linear model are defined by slopes of tangents to the nonlinear model trajectory in phase space. Unlike simple linear analytical models, TLM coefficients are therefore generally time dependent and are determined for realistic and complicated spatial structures.

A TLM has several important uses. Most directly it can be used to determine the evolution of small perturbations of fields in a model forecast, for example in a predictability or case study. More importantly, however, it can be used for propagating error statistics in Kalman filtering or for developing adjoint models for sensitivity studies or data assimilation. While development of a TLM is not strictly necessary for many of the latter applications, it is useful for understanding the inaccuracies of applications of its corresponding adjoint because the accuracies of both are strongly related, and it is usually easier to think in terms of a forward model of perturbation evolution (as in a TLM) than a backward model of sensitivities (as in an adjoint).

A TLM is intended to approximately describe the evolution of the small differences between two nonlinear model solutions when one solution begins from perturbed initial or boundary conditions or model parameters. If all model terms are differentiable with respect to the model fields and the exact unperturbed model solution is used to

* Corresponding author.
[1] The National Center for Atmospheric Research is sponsored by the National Science Foundation.

determine values of the TLM coefficients, then the TLM solution is asymptotic to the solution obtained as a difference between the two complete model solutions, as the perturbation magnitude tends toward zero. For perturbations the size of uncertainties in initial or boundary conditions or model parameters, the TLM solution is only an approximation to the true solution (unless the original model is also linear). Also, for many models, the TLM and difference solutions may eventually diverge, even for very small initial perturbations, due to mechanisms of predictability error growth that can increase the perturbation magnitude with time.

Besides the approximation due to linearization, there are two other causes of inaccuracy in some TLMs. One is due to the necessity of approximating or neglecting some model terms prior to linearization because either these terms are not differentiable, as is sometimes the case in physical parameterization schemes, or the second derivatives of model terms with respect to the model state variables are very large, so the linearization is useless. The other inaccuracy is due to approximating the true time evolution of the basic state by infrequently changing or temporally interpolating the basic state so that the TLM coefficients are only approximations to the true tangent slopes. This latter approximation is sometimes necessary for economy of computation or data storage.

A TLM may be considered accurate as long as the linearization is performed properly and completely, and its solutions are therefore truly asymptotically correct. Instead, however, we take a broader view that a TLM is primarily intended to approximate the evolution of perturbations in a corresponding nonlinear model, and therefore consider a TLM accuracy to be a measure of its performance in that regard. Similarly, an adjoint model may be considered to be totally accurate if it properly and exactly computes gradients of the form $\partial J/\partial x_i$, where J is a scalar measure of some forecast aspect, and x_i is the value of a model field at some point. If, however, we again take a broader view that the more common interest is in values of $\Delta J/\Delta x_i$ (i.e., for finite rather than infinitesimal perturbations of x_i), then we may also speak of the accuracy of an adjoint model as a measure of its performance in describing how a J would actually change due to perturbations in the corresponding nonlinear model. The meaning of the accuracy of these models in this paper will therefore not refer to their asymptotic behavior (which we regard as referring to the correctness of their formulation) but instead to their behavior for finite-amplitude perturbations. This meaning is analogous to that for most models in general, where it is not so much their correct formulation which defines their accuracy as it is their general results and applications.

In this paper, the accuracy (in the sense just described) of a TLM developed for a dry version of the PSU/NCAR mesoscale model (denoted MM4) is investigated. A dry version is used because we do not want to add the complexity and increased errors due to effects of highly nonlinear and discontinuous moist diabatic physical parameterizations. We determine the accuracy of this TLM as a function of: perturbation magnitude and structure, forecast period, frequency of basic state update, and synoptic case. In particular, we determine its accuracy for initial condition perturbations whose magnitudes are the size of expected analysis errors. If the TLM is accurate only when the perturbations size is much smaller, its usefulness would be more limited.

The accuracy of a TLM is necessarily dependent on the physics being described, which in meteorological problems depend on the spatial scales, processes, and cases being studied. We report results for our TLM because they indicate accuracy for not only adjoint applications we will describe in the future, but also for other models applied to similar problems (insofar as the modeled physics is similar). The results indicate the degree of accuracy that should be expected in other TLM development, as well as what approximations may be appropriate. They also provide a benchmark for our future study with a moist model.

The paper begins with a description of pertinent details about the MM4 and the corresponding TLM. The synoptic cases are described in Section 3 along with the methods for creating perturbations used in the testing. This is followed by Sections 4 to 6, respectively, describing results of each of the accuracy tests to which the TLM has been subjected. An accuracy test of the corresponding adjoint model is described in Section 7. A summary and some recommendations are offered in the concluding section.

2. Description of MM4 and its TLM

The MM4 is a limited-area, primitive equation model in flux form originated by Anthes and Warner (1978) and further developed by Anthes et al. (1987). It uses a Lambert conformal map on an Arakawa B grid. For numerical treatment of the lateral boundaries it uses a Davies and Turner (1977) scheme. It uses a Brown and Campana (1978) time scheme with an Asselin (1972) filter to control computational modes (time splitting). The vertical coordinate is $\sigma = (p - p_t)/p^*$, with $p^* = p_s - p_t$ for p pressure, p_s surface pressure, and p_t a prescribed top pressure (equal to 100 hPa in the experiments reported here).

The physical parameterizations included in this study are: a Deardorff (1972) bulk aerodynamic formulation of the planetary boundary layer, a Richardson number dependent vertical diffusion, and both 4th order and 2nd order horizontal diffusion (applied in the interior and near the lateral boundaries, respectively) with prescribed diffusion coefficients. Ground temperature is prognostically determined with radiative fluxes computed every 30 minutes.

An earlier TLM was developed for MM4 as described in Errico and Vukićević (1992). It was based on a reformulation of the MM4 equations in a non-flux form and neglected several terms that arise from a complete linearization of the MM4 (e.g., it neglected the effects of p_s perturbations on computation of the perturbed geopotential and effects of perturbations of the density on the perturbed vertical diffusion). Even with its several neglected terms, it produced good approximations to the evolution of perturbations for forecast periods between 6 and 36 h. It did not yield truly asymptotic solutions, of course, and some fields had noticeable errors (e.g., gravity wave perturbations had incorrect phase speeds at some spatial scales).

The current dry version of the TLM is exact in the sense that it asymptotically yields the solution of a difference between MM4 solutions as the perturbation magnitude tends toward zero, except for the effects of four approximations:

(1) Perturbations of the coefficients of the Richardson-number dependent vertical diffusion are ignored by the TLM. Actually, these coefficients often have their maximum or minimum permitted values implying their perturbations are in fact zero, so this approximation is often negligible in practice.

(2) Perturbations of p_s are ignored in the determination of the difference between potential temperatures of the ground and the lowest model level when used to calculate the diabatic vertical fluxes of u, v, T, and moisture q, although it is used to convert temperature to potential temperature elsewhere.

(3) There is no consideration of dry convective adjustment by the TLM, although it can occur in the MM4. In many cases it occurs infrequently or not at all.

(4) The basic state used to compute the TLM coefficients is varied discontinuously by periodically reading fields from a stored file and computing coefficients at those times accordingly. The coefficients are held constant between these periodic basic state updates. Since the MM4 time step is determined by numerical stability considerations, the short scales often considered require very short time steps, and therefore, storage and input of all fields at every time step for an extended period is a prohibitive cost on most existing computer systems. Additionally, some computational savings are obtained since all coefficients need not be recomputed every time step. The impact of this approximation is explored in Section 6.

3. Synoptic situations

Two very different synoptic situations are considered. They were selected because the typical wind speeds and magnitudes of temperature and pressure gradients differed significantly. These are the same conditions selected in the examination of mesoscale dynamic balance by Errico (1990).

The initial conditions come from the European Center for Medium-Range Weather Forecasts (ECMWF) First GARP Global Experiment (FGGE) analyses archived at the National Center for Atmospheric Research (NCAR) and interpolated to the MM4 grid. That grid consists of 101×76 points oriented approximately east–west $\times$ north–south, centered at 40° N and 90° W with a grid spacing of 50 km. There are 10 vertical levels, equally spaced in σ, in addition to the surface. Lateral boundary values are specified as a function of time from the same spatially

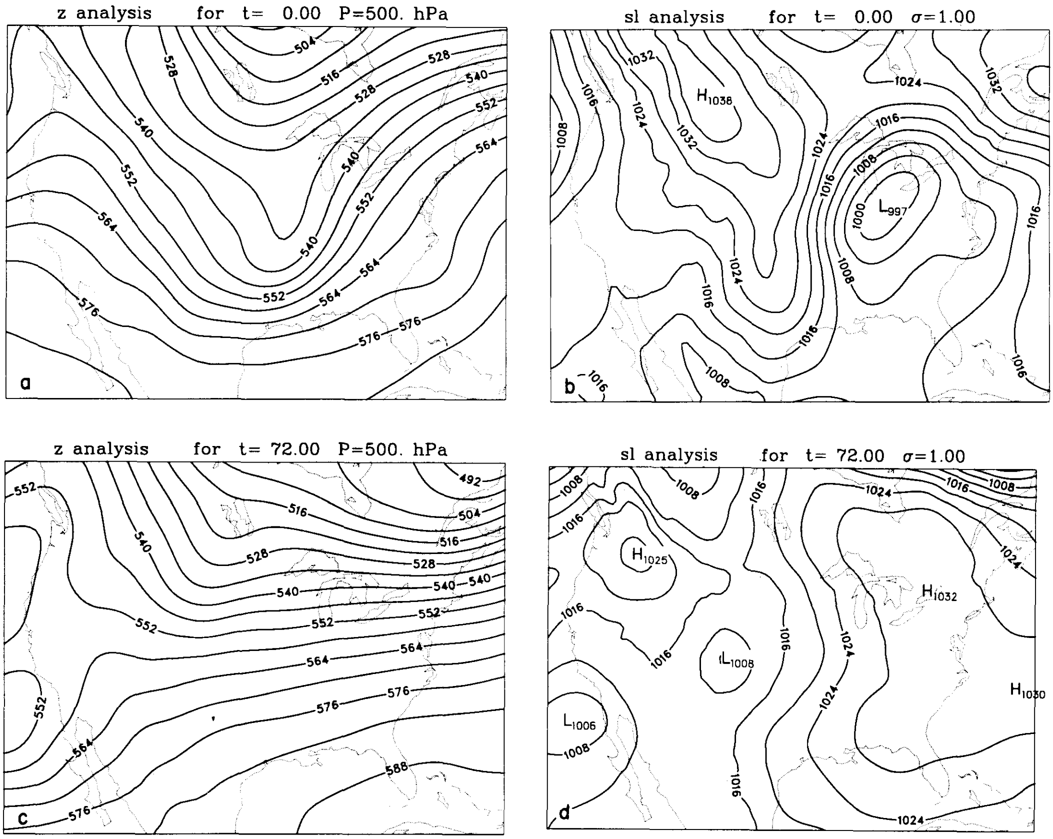

Fig. 1. The fields of 500 hPa geopotential height and sea-level pressure at the beginning (0000 UTC 14 January 1979; hour 0) and end (hour 72) of the winter case as interpolated to the MM4 grid from the ECMWF analyses. Units are dam and hPa, respectively.

interpolated ECMWF analyses with an additional temporal linear interpolation between 12-hourly fields. Integrations of both the MM4 and TLM are performed with a one-minute time step.

The winter case covers the period between 0000 UTC 14 January and 0000 UTC 17 January 1979. The fields of 500 hPa geopotential height and sea-level pressure at the beginning and end of this period appear in Fig. 1. At the initial time a surface cyclone centered over Indiana and an associated upstream, upper-level trough dominate the fields. These rapidly propagate eastward until hour 48 (not shown) where the surface is dominated by anticyclones over the north central and southeast portions of the domain with the upper level flow nearly zonal (with a slight southerly component except in the northwest quadrant of the domain). At hour 72 the surface anticyclones have propagated eastward and a new cyclone is developing over Colorado, while a 500 hPa trough appears over Montana.

The summer case covers the period between 0000 UTC 18 July and 0000 UTC 21 July 1979. The fields of 500 hPa geopotential height and sea-level pressure at the beginning and end of this period appear in Fig. 2. Throughout this period the 500 hPa flow is characterized by a quasi-stationary wave with a trough over Minnesota and a ridge over Idaho. The surface pressure field is dominated by an anticyclone that slowly propagates eastward.

The TLM is tested by considering random perturbations. Each field at each grid point and level is assigned a perturbation value randomly selected

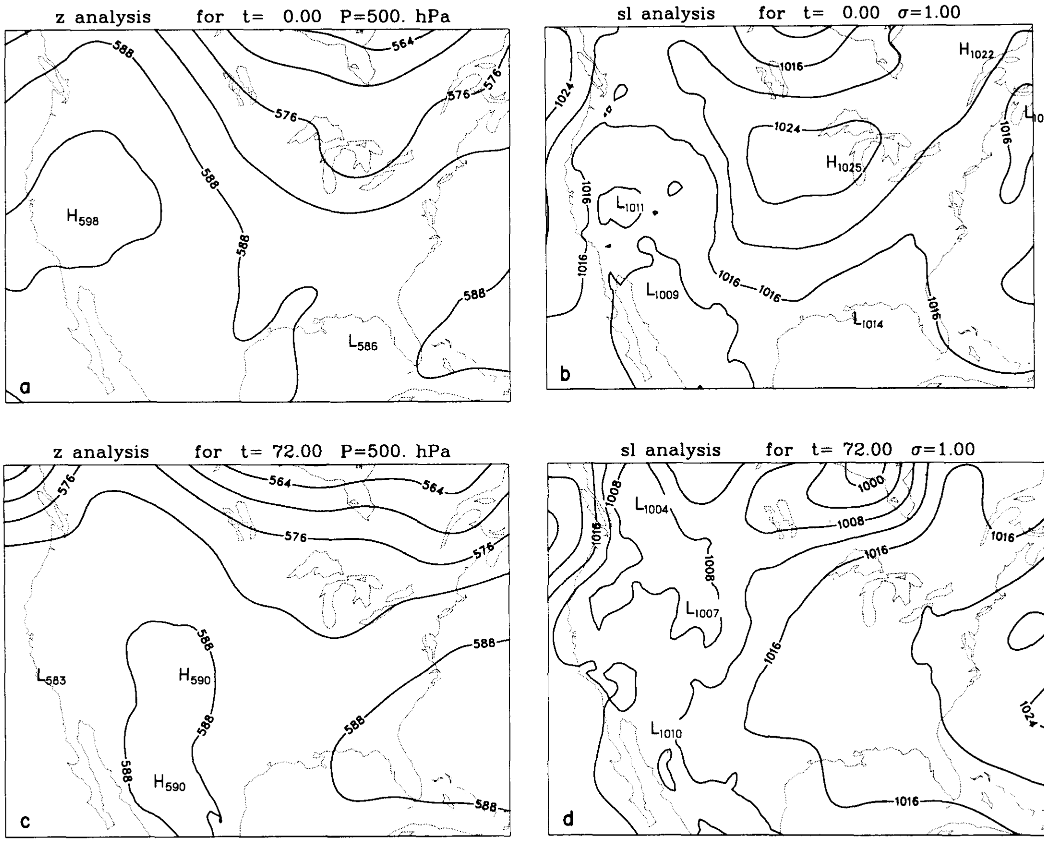

Fig. 2. Same as Fig. 1, except the summer case begins 0000 UTC 18 July 1979.

from a uniform distribution between $\pm PX$, where P is a common scaling factor and the value of X depends on the type of field: $3\ \mathrm{ms}^{-1}$ for u and v (eastward and northward wind components), 1 K for T (temperature), and 1 hPa for p_s (surface pressure). Perturbations for wind and temperature are further scaled by a factor of $p^* = 10^3$ hPa to put values directly in flux form (e.g., perturbations of p^*u). The values of X were chosen to reflect the ratios of current analysis error magnitudes for different fields. The externally provided, lateral boundary values required by the Davies and Turner (1977) scheme are not perturbed.

4. Accuracy of tendencies

As a first test of the TLM software, the asymptotic behavior of the model terms that comprise its tendency equations must be ensured. Here we not only do that, but also describe the accuracy of the TLM for perturbation magnitudes that are more the size of current analysis errors.

The basic state at hour 0 for either of our cases is simply given by our interpolated analyses. This state is neither geostrophically adjusted nor consistent with the model horizontal diffusion (Errico, 1990). For the tendency accuracy estimates, the fields produced by a 24-hour model forecast are used as the basic state to which perturbations are applied. This state has been dynamically adjusted in a natural way by the model processes that have acted upon it during the forecast.

The random perturbations described in Section 3 have two characteristics which make them extremely unlike typical analysis errors: they have no spatial correlation, either horizontally or vertically; and they are dominated by ageostrophic features since there are no prescribed relationships between fields (aside from maximum permissible values). For these reasons, in short period forecasts, the dynamics of these perturbations should be dominated by the damping process of diffusion and the propagation characteristic of inertial gravity waves. Both of these processes should be well modeled by a linear model since their dominant physics is quasi-linear. These perturbations, therefore, do not provide a good test of the TLM tendency accuracy.

In order to obtain accuracy estimates from more realistic perturbations that are more strongly affected by nonlinearity, an additional type of perturbation was constructed. For this perturbation, spatial correlations and correlations between fields were produced by making a 12-h forecast with the TLM using as a basic state hours 12–24 of the MM4 forecast and using as an initial perturbation random fields specified as in Section 2 (except with the values of X equal to 1 ms^{-1}, 1 K, and 1 hPa for wind, temperature, and pressure, respectively). The effect of the TLM forecast is to damp small scales and geostrophically adjust fields as the MM4 would so that the perturbation fields produced at the end of the forecast have the desired correlations.

As a consequence of the adjustment and damping, the magnitudes of the perturbation fields have been reduced and, therefore, prior to their application as a perturbation (at basic state hour 24), these perturbations are normalized by multiplying all fields by a single factor (2.27 in the winter case; 3.1 in the summer), so that the resulting maximum absolute value of the surface pressure perturbation is 1 hPa as before. For the winter case, the resulting maximum magnitudes of the perturbation fields are 6.6 ms^{-1}, 1.6 K, 1 hPa and the rms values are 0.8 ms^{-1}, 0.3, and 0.2 hPa. This perturbation is denoted as the filtered perturbation of scale $P = 1$. For the summer case, these corresponding measures are slightly larger.

The correlated p_s perturbation field for the winter case is shown in Fig. 3. The typical length scale between relative maximum values is approximately 1000 km. The lack of perturbations near the western boundary is a consequence of the sweeping effect of advection from the western (inflow) boundary when the perturbation there is specified as zero (Errico and Baumhefner, 1987).

As a measure of accuracy, we compute the correlation between corresponding perturbation tendencies determined from the TLM and from the difference between nonlinearly computed (basic state and perturbed) tendencies. The correlations are computed as averages over all points (vertically and horizontally) excluding the domain edges that are specified as having zero perturbation. Actually presented is the correlation error (E_c

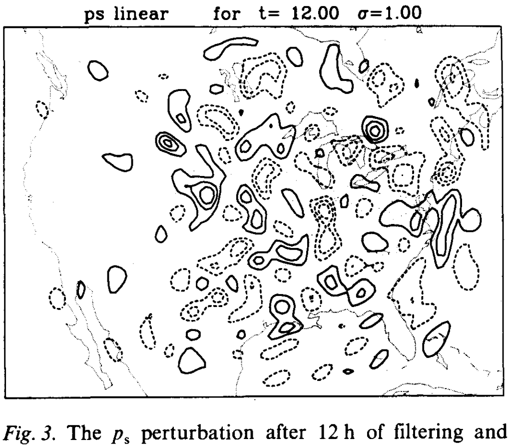

Fig. 3. The p_s perturbation after 12 h of filtering and adjustment by the TLM and renormalization. The contour interval is 0.25 hPa, negative-valued contours are dashed and the zero-valued contour is omitted.

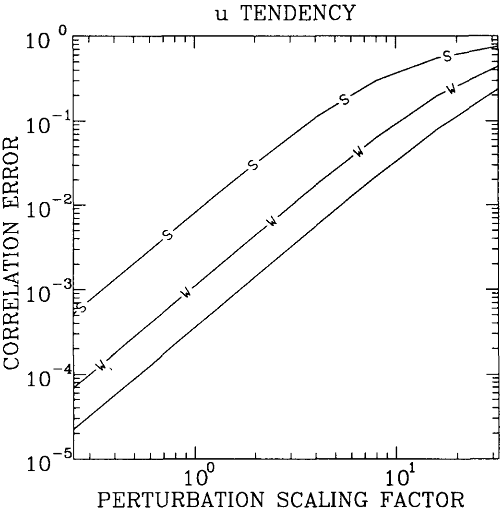

Fig. 4. Correlation error of the u tendencies as a function of the perturbation scaling parameter P. Labels W and S denote results for the correlated perturbations applied to the winter and summer cases respectively. The solid line is for the random perturbation applied to the winter case.

equal to 1 minus the tendency correlation) as a function of the scaling factor P applied to the basic perturbation. Results for the u, v, and T tendency fields are all similar, so only those for u are shown in Fig. 4.

For the winter case with the filtered perturbation, $E_c = 0.001$ for the basic perturbation ($P = 1$). This error corresponds to greater than two-digit accuracy for tendency calculations of fields at individual points (except perhaps where values are relatively very small). For the winter unfiltered perturbation (produced as the random perturbation described in this section, but applied to hour 24), E_c is one third that value for reasons described earlier. For the summer case, $E_c = 0.07$. There are three likely reasons for this increase in error for the summer case, which, in order of importance, are: (1) the basic state is significantly weaker (winds half as large) that implies perturbations of identical magnitudes would be *relatively* larger; (2) the perturbation of u, v, and T is slightly (30%) larger due to the normalization factor being larger; and (3) area mean measures (e.g., rms) of the perturbation are also increased because the sweeping effect in the summer cases is weaker than in winter due to the weaker wind speeds. For $P \leqslant 4$, $E_c \propto P^2$ which is the asymptotic relationship describing the neglect of quadratic perturbation terms by the TLM.

These results indicate that perturbations that have the magnitude of analysis errors ($P < 4$) do indeed fall within a quasi-linear regime for the perturbation tendencies for a typical winter case. Perturbation tendencies are computed sufficiently accurately for most purposes. For the summer case, this is probably not true for $P \geqslant 2$.

5. Accuracy of time integration

Although the TLM computes perturbation tendencies accurately, it is not obvious that an integration over an extended time will produce accurate perturbation fields. The tendencies are neither a random walk (which would cause much cancellation of errors from one time step to another) nor a systematic forcing (which would scale errors proportional to time). Here we will show the magnitudes and characteristics of errors in perturbations during 72-h forecasts. The initial perturbation is that described in Section 2 (identical perturbations for both winter and summer cases). The basic state is updated every 6 minutes for these experiments.

5.1. *Winter case*

The correlations of the u, v, T, and p_s fields as functions of time for the winter case appear in Fig. 5. During the first 18 h, the correlations of all fields decay to 0.98. This decay is expected since errors should compound in some way. During the remaining 54 h, the fluctuations are greater, but the decay is slower, settling near 0.97. This behavior is more unexpected. The magnitude of the perturbation decays with time, as is frequently the case in predictability studies with the MM4 (Errico and Baumhefner, 1987, Vukićević and Errico, 1990); and this would act to reduce the errors with which perturbation tendencies are calculated, thereby slowing the rate of error growth for the field correlations. Also, the boundary sweeping effect will change the characters of the fields that are being correlated.

Correlations do not vary greatly with σ-level at any time (supporting results are not shown), but for each field, the lowest level usually has the smallest correlation. This may be due to one of the approximations (i.e., departures from an exact linearization) made in the TLM, but more likely is due to the fact that the magnitude of the wind perturbations near the surface are larger relative to

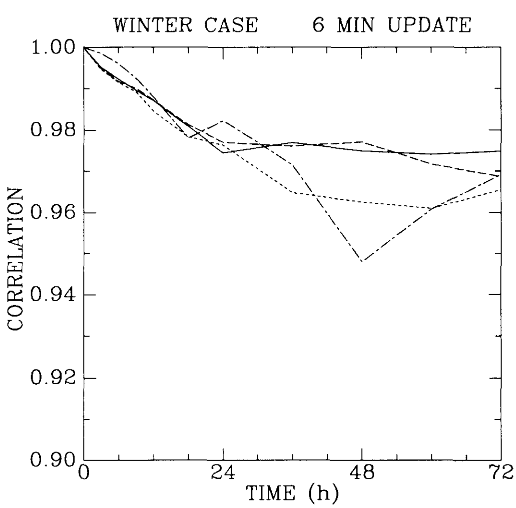

Fig. 5. Correlations of the u (solid), v (long dash), T (short dash) and p_s (alternating long, short dash pattern) perturbation fields for the winter case.

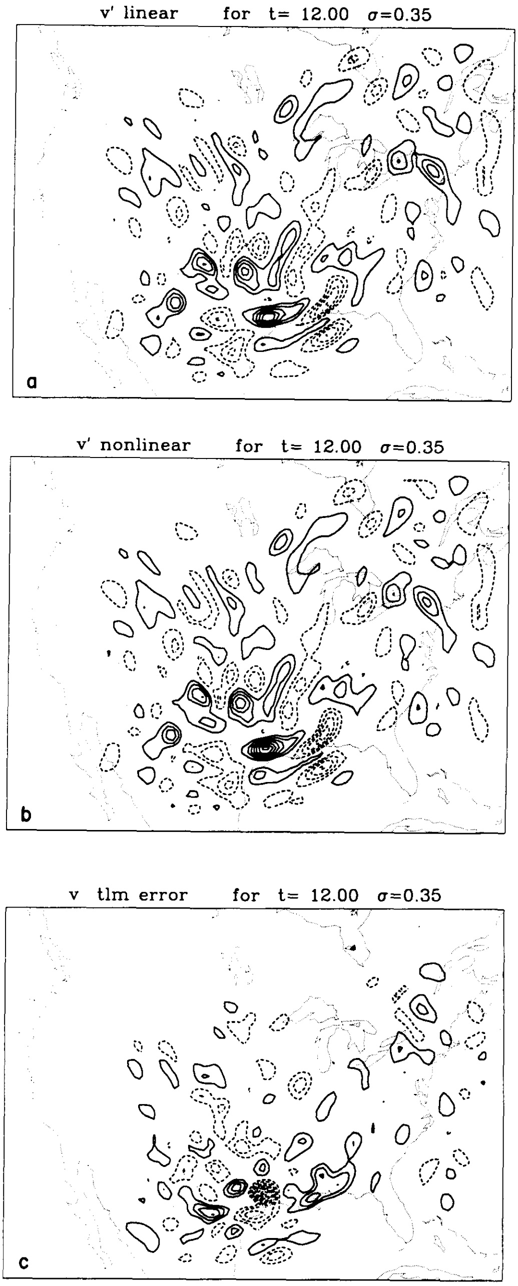

Fig. 6. Perturbations of v on the $\sigma = 0.35$ surface at forecast hour 24 computed by (a) the TLM and (b) as a difference between nonlinear forecasts and (c) the difference between the two fields. The contour interval is (a–b) $0.5\ \mathrm{ms}^{-1}$ and (c) $0.1\ \mathrm{ms}^{-1}$. Negative-valued contours are dashed and zero-valued contours are omitted.

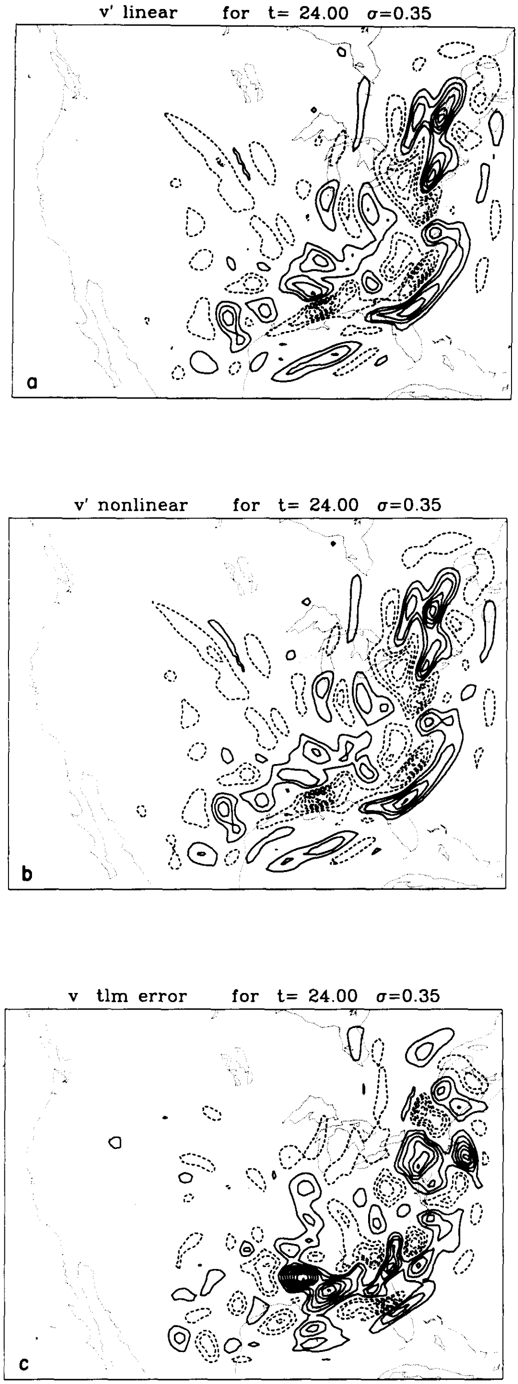

Fig. 7. As for Fig. 6, but at forecast hour 24 with contour intervals (a–b) $0.25\ \mathrm{ms}^{-1}$ and (c) $0.05\ \mathrm{ms}^{-1}$.

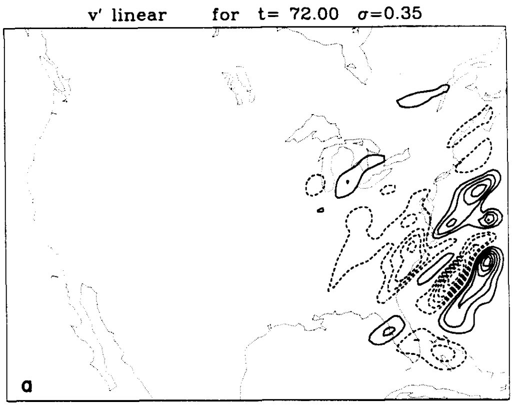

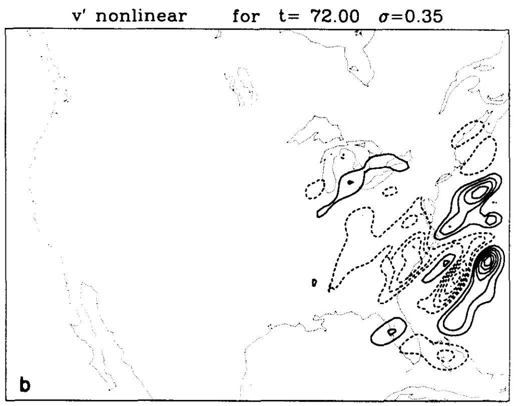

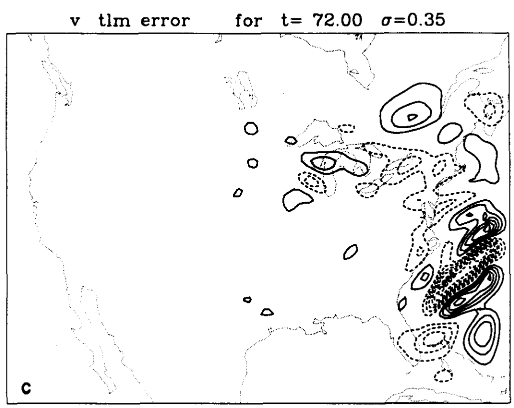

Fig. 8. As for Fig. 6, but at forecast hour 72 with contour intervals (a–b) 0.05 ms^{-1} and (c) 0.01 ms^{-1}.

the basic state field at that level than are the relative magnitudes at other levels. It is the relative magnitude which determines the accuracy of the linearization when measured as a correlation. When the errors are measured in terms of rms, standard deviation, or maximum absolute value, the velocity field TLM errors are greatest in mid-troposphere, but the temperature errors are usually still greatest in the lower troposphere.

Some characteristics of the TLM errors are revealed by comparing perturbation fields forecast by the TLM with those computed as differences (denoted as ND) between two nonlinear forecasts. As an example, the v field perturbations on the $\sigma = 0.35$ surface are presented. The characteristics to be described are similar at other levels and for other fields. An error field computed as the difference between the TLM and nonlinear produced fields is also presented.

Results for hour 12 appear in Fig. 6. Note that the model's sponge near the lateral boundaries has acted to remove perturbations there (except in the northeast where the boundary condition is outflow). The TLM and ND fields look quite similar (correlation 0.987) even with regard to small details. The rms values of the TLM and ND fields are both 0.43 ms^{-1}, and the rms value of the error field is only 16% of that value (the contour interval used for it is five times smaller than for the others). For the ND field, the maximum value is

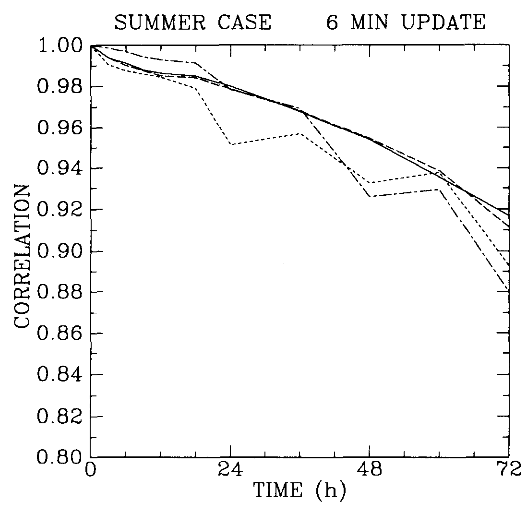

Fig. 9. As for Fig. 5, except for the summer case.

3.69 ms^{-1} near Houston, Texas, while in the TLM field it is 2.99 ms^{-1} and 50 km further to the south. The maximum absolute error is located in the same vicinity.

The boundary sweeping effect is even more evident for hour 24, shown in Fig. 7, with most of the perturbation aligned along the east coast of the US. The correlation of the TLM and ND fields is 0.978 and their rms values have both decreased by 40% of their values at hour 12 (primarily due to the sweeping affect). The error field does not have the same structure as the TLM or ND fields, but it has the same spatial scale, indicating the errors are dominated by neither phase nor amplitude errors alone.

By hour 72 (Fig. 8) all significant perturbation is in the eastern quarter of the domain. The rms and maximum values of the perturbation fields have been reduced greatly since hour 24 (the latter to a value of only 0.35 ms^{-1}). The correlation between the TLM and ND fields remains high at 0.973. The maximum magnitude of the error field is one quarter the maximum perturbation value. The error field appears to be dominated by magnitude errors since the structures of all three fields are similar, and the larger maximum and minimum values of the TLM and ND fields appear colocated. The reduction of the magnitude of the perturbation itself has likely contributed to the sustaining of the high correlations.

5.2. Summer case

Correlations of the u, v, T, and p_s fields as functions of time appear in Fig. 9. Values drop more steadily in time compared with the summer case. By hour 72, they are near 0.90. This result agrees with those for the tendency calculation which also shows greater errors for the summer case. It is also likely affected by the magnitude of the errors, which is also greater than the winter case because, as will be shown, the boundary sweeping effect is weaker.

The TLM v field for $\sigma = 0.35$ at hour 24 and its associated error field are presented in Fig. 10. Note that boundary damping has occurred in the sponge region, but the only apparent sweeping effect is over Canada. The rms value for the TLM field is 70% that for the winter case at the same time, but the maximum absolute values of corresponding fields for the two cases are similar. The

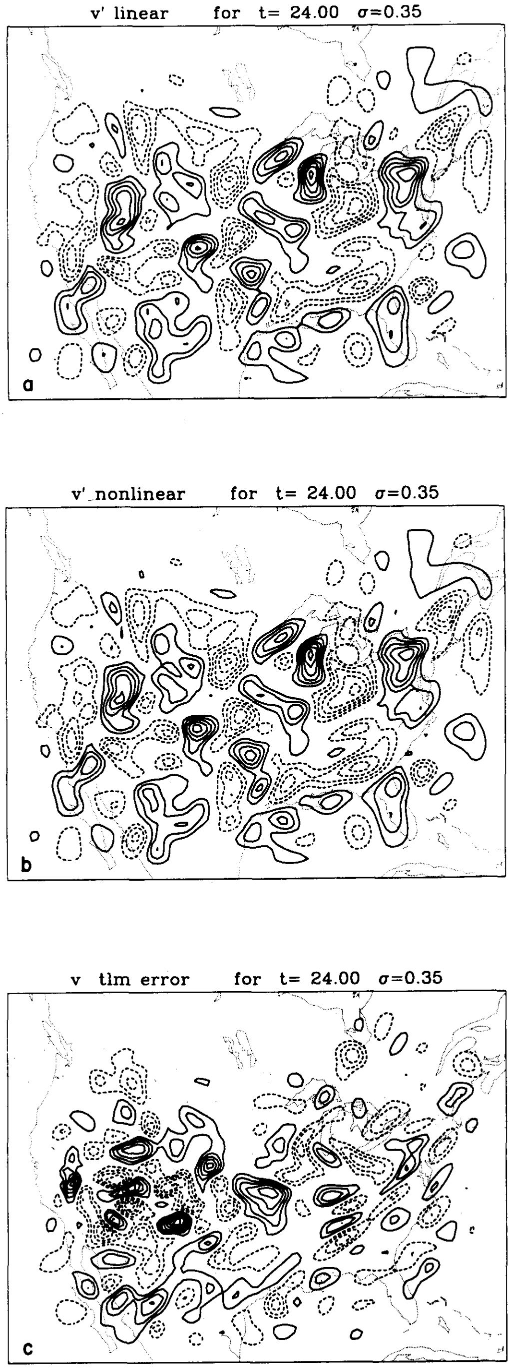

Fig. 10. As for Fig. 6, but for the summer case at forecast hour 24 with contour intervals (a–b) 0.25 ms^{-1} and (c) 0.05 ms^{-1}.

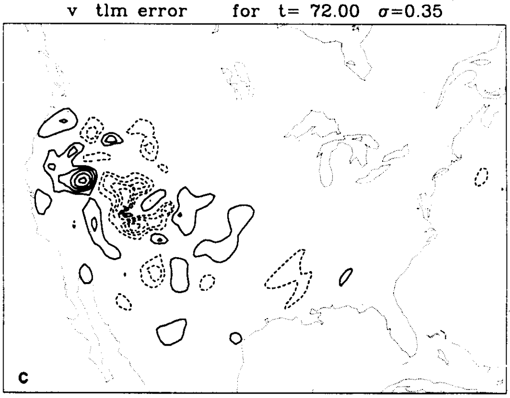

Fig. 11. As for Fig. 6, but for the summer case at forecast hour 72 with a contour interval 0.1 ms^{-1}.

rms and maximum absolute values for the error field are approximately one-fifth their TLM values.

Corresponding figures for hour 72 appear in Fig. 11. The sweeping effect is still not great. Magnitudes and rms values for the TLM field have decreased compared with those at hour 24, but not as much as for the winter case. The maximum absolute value for the error field is now 70% that for the TLM field. When correlations as low as 0.90 were obtained for other experiments, ratios of maximum absolute values similar to this were also obtained. The correlation measure of the accuracy tends to suggest closer agreement between figures than some other measures do.

6. Accuracy of infrequent update

The results in the last section suggest that for many applications, the basic state does not need to be updated every time step. Aside from the few minor neglected terms in the TLM development, the TLM error is due to the neglect of second and higher-order perturbation terms and the infrequent update.

The exact effect of perturbations of fields u and v on a quadratic term uv at time t would be

$$E = (\bar{u}_t + u'_t)(\bar{v}_t + v'_t) - \bar{u}_t \bar{v}_t, \tag{1}$$

where the overbar denotes a basic state or control forecast and primes denote perturbations. The TLM approximation using a basic state at time t_n would be

$$A = \bar{v}_{t_n} u'_t + \bar{u}_{t_n} v'_t, \tag{2}$$

yielding an error

$$E - A = (\bar{v}_t - \bar{v}_{t_n})\, u'_t + (\bar{u}_t - \bar{u}_{t_n})\, v'_t + u'_t v'_t. \tag{3}$$

The expressions in parenthesis may be approximated by, e.g.,

$$(\bar{v}_t - \bar{v}_{t_n}) = \frac{\partial v}{\partial t}\, \Delta t, \tag{4}$$

where $\Delta t = t - t_n$ is not greater than the update period. For large perturbation magnitudes and small update periods, the last term in eq. (3) will dominate, but for large update periods, the first two terms will dominate and the error will then be linear in the perturbation magnitudes. For small perturbations, the error will become small, but the TLM and ND solutions will not be asymptotic because the first two terms in eq. (3) are essentially additional linear terms.

To demonstrate that the update period can be quite long for many purposes, the experiments in Section 5 were repeated using the identical design except with longer update periods. The correlations of the u, v, T, and p_s fields as functions of time for these two new experiments appear in Figs. 12 and 13 for the winter and summer cases, respectively.

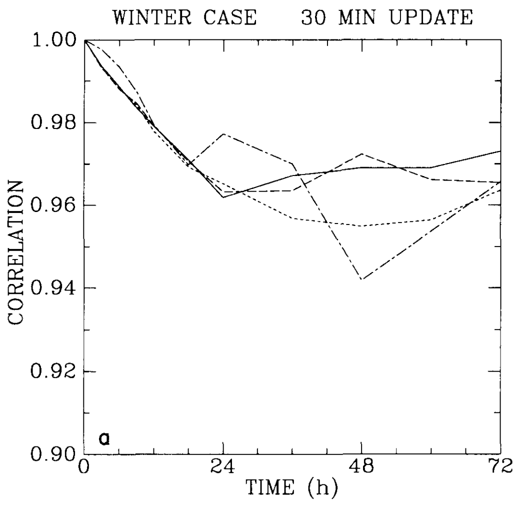

For the winter case, during the first 18 h with the 30 min update, the correlations of all fields decay only slightly faster than for the 6 min experiment (Fig. 5), and the values at hour 72 are not significantly different between the experiments. If the update period error dominated, we would expect the error to scale with the ratio of update periods. Since this is far from the case, we conclude that the error between these two experiments is dominated by the neglect of nonlinear perturbation terms by the TLM. The fact that changes of the update period appear more important during the first 18 h than subsequently is likely due to the fact that the forecasts are noisy initially (i.e., when strong gravity waves and damping are present) and the tendencies in eq. (4) are larger.

For the winter case with 90-min update, during the first 18 h, the correlation drops about three times faster than for the 30-min update, suggesting that the error is now dominated by the infrequent update. At hour 72 (as well as at hour 18), the correlations are near 0.9. With correlations this low, at the locations of local maximums and minimums in the TLM fields, errors as large as 70% are observed (analogous to those shown in Fig. 11). For some quantitative applications, the TLM with this update period applied to a case such as this would be inadequate, although

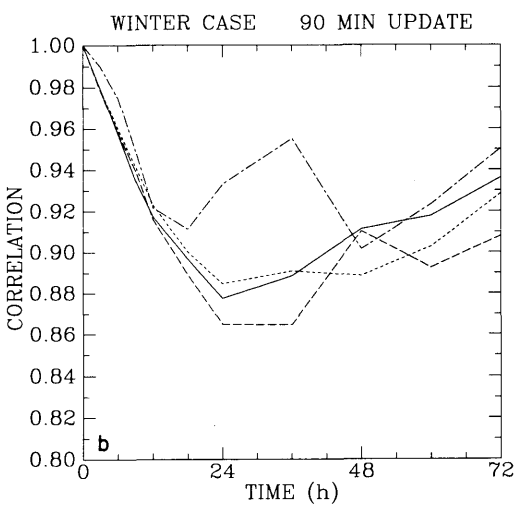

Fig. 12. As for Fig. 5, except for update periods (a) 30 min and (b) 90 min.

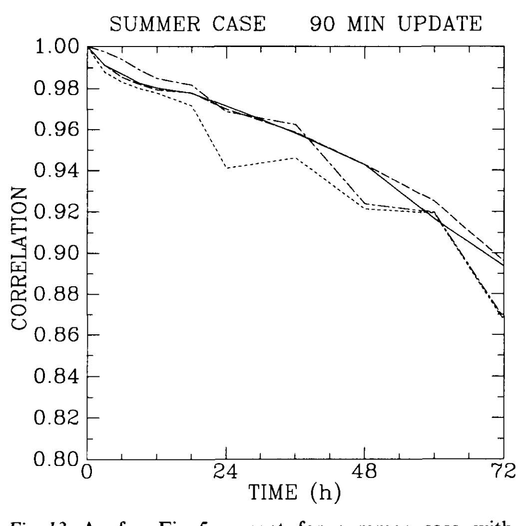

Fig. 13. As for Fig. 5, except for summer case with update period 90 min.

qualitatively the results (both figures and perturbation statistics) are quite similar.

For a perturbation one-tenth the size of the previous experiments, the relative agreement between the 6- and 30-min update TLM solutions after hour 24 diminishes. For such a small perturbation, the nonlinear perturbation errors still dominate for the first day (and the errors are observed to scale quadratically with the perturbation magnitude), but thereafter, as the perturbation decays with time, the perturbations become sufficiently small (e.g., u' values less than $0.1\ \mathrm{ms}^{-1}$) that the update infrequency error dominates. After this latter event occurs, the errors become linear in perturbation magnitude and the correlation errors no longer become smaller as the perturbation size decreases further.

For the summer case, all error statistics for the 6- and 90-min update period experiments are similar (with those for the latter typically slightly worse). Corresponding fields look greatly alike, including the error fields. This indicates that the TLM error for this case is not dominated by the infrequency of the update, even for periods as long as 90 min. Essentially, when the synoptic evolution is quite slow, an update period as long as 90 min appears adequate. This result may not apply if some rapidly changing physical process, such as is possible with moist convection, was added to the simulation. Neither may it apply if the magnitude of the perturbation is substantially reduced.

7. Accuracy of adjoint model

In a particular sense, the accuracy of the adjoint model that corresponds to the TLM is identical to that of the TLM. This can easily be seen by following the adjoint development in Errico and Vukićević (1992). Denote J' as a first-order approximation to the change of a measure of some forecast aspect, x'_0 as an initial TLM state vector, $\hat{x}_t$ the gradient of J with respect to the forecast state vector at time t, and A_t as the propagator matrix of the TLM. Then

$$J' = \hat{x}_t^{\mathrm{T}} A_t x'_0 = x_0'^{\mathrm{T}} A_t^{\mathrm{T}} \hat{x}_t, \tag{5}$$

where superscript $^{\mathrm{T}}$ denotes a transpose; i.e., given either x'_0 or $\hat{x}_t$ (which may both be considered as prescribed) then identical values of J' are obtained whether the TLM or adjoint models are applied, implying both values are equally accurate, even when finite-amplitude perturbations are considered.

Still, it is worthwhile to provide an example of the accuracy of an adjoint calculation, especially since we will claim that the accuracy is much better than we, or most others, would have expected. We use as our adjoint one that is exactly that of our TLM. For our example, we consider J to be the area mean vorticity within a circle of radius 150 km positioned at the center of the model grid and vertically averaged throughout the model depth:

$$J = \frac{1}{N} \sum_{i,j,k} \Delta\sigma_k \zeta_{i,j,k}, \tag{6}$$

where $N = 29$ is the number of grid points within the circle, the sum is over horizontal points i, j lying in the circle, $\Delta\sigma_k$ is the depth of the kth sigma level, and ζ is the vorticity determined as a function of u and v (which include values at points outside the circle, since ζ depends on the gradients of those fields). According to Stoke's Theorem, J is proportional to the barotropic circulation integrated around the same circle. The time at which J is to be verified is hour 72 of the winter case.

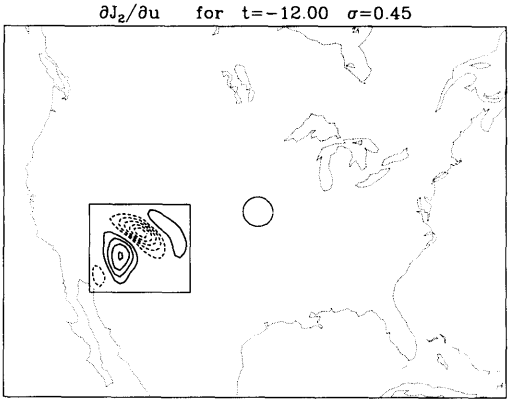

Fig. 14. The sensitivity of J with respect to initial u perturbations on the $\sigma = 0.45$ surface 12 h prior to verification. The contour interval is $5 \times 10^{-5}\ \mathrm{sm}^{-1}$, negative-valued contours are dashed, and zero-valued contours are omitted. The circle indicates the region where J is calculated. The box indicates where subsequent perturbations are applied.

The adjoint begins with values of $\partial J/\partial u$ and $\partial J/\partial v$ determined by consideration of eq. (6) and the functional expression for ζ at each grid point. The adjoint equations are then applied recursively backward in time to obtain the gradient of J with respect to all field values at an initial time 12 h prior to the verification time. The resulting field of $\partial J/\partial u$ on the $\sigma = 0.45$ surface at this initial time is presented in Fig. 14 as an example. It was computed using a basic state update period of 90 min. Note that the greatest sensitivity is in a small region upwind from the verification area.

The adjoint results are applicable to any perturbation. In order to select one perturbation for the accuracy test, we have chosen to perturb all u and v components within a box (see Fig. 14) at all vertical levels with a structure identical to that of the corresponding adjoint fields, but scaled so the maximum magnitude of either component is $3\ \mathrm{ms}^{-1}$. Initially, outside the box, perturbations are zero and no other fields are perturbed.

The perturbation was applied to a 12-h nonlinear forecast begun from hour 60 of our analyzed data. The change in J computed at hour 72 (denoted ΔJ) between this perturbed forecast and a similar control forecast was then contrasted with the value J' computed from the adjoint fields themselves, as in the second equation in eq. (5). The perturbation of u on the $\sigma = 0.45$ surface at hour 72 (computed as a difference between the nonlinear forecasts) is presented in Fig. 15. Note

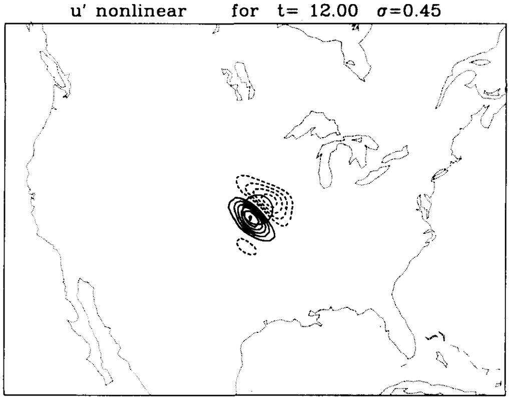

Fig. 15. Perturbations of u on the $\sigma = 0.45$ surface after a 12-h forecast produced as a difference between nonlinear solutions. The contour interval is $0.4\ \mathrm{ms}^{-1}$, negative-valued contours are dashed and zero-valued contours are omitted.

the perturbations extend to regions outside the circle where J is calculated.

For the experiment with maximum perturbation magnitude $3\ \mathrm{ms}^{-1}$ and basic state update period 90 min, $R = J'/\Delta J$ was 1.013. With an identical initial perturbation structure but scaled to yield a maximum value of $0.03\ \mathrm{ms}^{-1}$, a second perturbation forecast (expected to be more quasi-linear because the perturbation magnitudes are reduced by a factor of 100) yielded $R = 1.0076$. The error (0.0076) is presumably not reduced by a large factor because the error is dominated by the infrequent basic state update used to compute the gradient for the J' calculation. When the second experiment is repeated using the same perturbation but an update period of 15 min, $R = 1.0034$.

8. Conclusions

The perturbation tendencies computed by the adiabatic portion of the dry TLM are exactly asymptotic to the true perturbation tendencies determined as differences between nonlinear calculations. Even for perturbations as large as current analysis errors, correlations are as high as 0.995 for a typical winter case. In summer, correlations are smaller because, for a similar magnitude perturbation, values relative to the unperturbed temperature and pressure gradients and wind fields are larger.

The correlations of TLM and nonlinearly perturbed fields decay as a forecast proceeds, until the rates of error removal (by adjustment processes and error sweeping by the boundaries) dominate the rates of error growth (due to tendency errors). For our winter case, this transition occurred before hour 24. After hour 48 correlations actually increased, in part because not only is the sweeping effect quite large, but also the rate of error growth has been substantially reduced as the perturbation magnitude itself has decayed. For our summer case no transition was observed because both the errors in the tendencies are larger and the sweeping effect is weaker.

At the end of a 72-h forecast period, correlations for the winter case are as high as 0.96 and for the summer case 0.90. In terms of maximum absolute values of fields, this corresponds to a ratio of approximately five for perturbation to error values for the former case and two for the latter.

As the period for the update of the basic state was increased from 6 to 30 min, little change of the error fields or statistics was observed for perturbations as large as analysis errors. An exception is during the first 18 h of the forecast when (due to dynamic imbalances in the initial conditions) the tendencies of the control fields are large, and consequently, the changes of the basic state in time are large. Except during this adjustment period, the TLM error is dominated by the TLM neglect of terms that are nonlinear in perturbation fields, and the error due to infrequent update is negligible. For the summer case, 90 min was also a suitable update period, since the nonlinear errors are even more dominant. For smaller perturbations (approximately when the wind perturbation magnitudes were less than 0.1 ms^{-1}), the error due to updating as infrequently as every 30 min appeared to dominate the other errors.

An infrequent update can be a substantial savings on computational and file storage costs. For a mesoscale model that requires short time steps, the cost of updating the basic state every time step can be prohibitive for a forecast longer than 12 h. For our experiments, 3×10^5 field values must be stored and read each update time (equivalent to 10^{10} bytes for a 72-h forecast with every time step update). Our results suggest that, as long as perturbation magnitudes are not much smaller than one-thirtieth typical analysis errors, an update period as long as 10–30 min may be suitable, reducing our storage requirements by 10–30. In a moist case, where the timing of convection is a factor, shorter periods may be necessary. If only qualitative analysis of the TLM results are to be reported, then even longer update periods are suitable. It is recommended that either the shortest practical update period be used, or the magnitudes of the error terms in eq. (3) be estimated by considering a typical value of the tendencies in eq. (4).

The error in the TLM computation of a forecast aspect is identical to that for the adjoint. As a demonstration of our adjoint accuracy, we calculated the change of the mean barotropic vorticity within a region due to initial perturbations in the velocity field for a 12-h forecast. The adjoint result was computed as the inner product (projection) of the initial perturbation on the sensitivity field determined by the adjoint model. It was compared with the impact calculated as a difference between perturbed and controlled nonlinear forecasts. For a perturbation magnitude as large as 3 ms^{-1}, the impact was computed with less than 1% error.

Certainly, for any qualitative use, the TLM results appear identical to those computed as a difference between nonlinear forecasts for the kind of perturbations and synoptic situations we have considered. Furthermore, the TLM results should be sufficiently accurate for most quantitative uses as well. For a winter case this may be true even for a forecast as long as 72 hours. For summer cases, the limit may be shorter.

9. Acknowledgments

T. Vukićević and K. Raeder are funded through the National Aeronautics and Space Administration's (NASA) Earth Observing System (EOS) Interdisciplinary Science Investigation entitled "NCAR project to interface climate modeling on global and regional scales with EOS observations" working on problems and development of data assimilation. Participation at the Workshop on Adjoint Applications in Dynamic Meteorology was partially funded by NASA and NSF. The manuscript was prepared by Lydia Harper.

REFERENCES

Anthes, R. A. and Warner, T. T. 1978. Development of hydrodynamic models suitable for air pollution and other mesometeorological studies. *Mon. Wea. Rev. 106*, 1045–1078.

Anthes, R. A., Hsie, E.-Y. and Kuo, Y.-H. 1987. Description of the Penn State/NCAR Mesoscale Model Version 4 (MM4). NCAR Technical Note, NCAR/TN – 282 + STR, 66 pp. [Available from the National Center for Atmospheric Research, P.O. Box 3000, Boulder, CO 80307, USA.]

Asselin, R. 1972. Frequency filter for time integration. *Mon. Wea. Rev. 100*, 487–490.

Brown, J. and Campana, K. 1978. An economical time–differencing system for numerical weather prediction. *Mon. Wea. Rev. 106*, 1125–1136.

Davies, H. C. and Turner, R. E. 1977. Updating prediction models by dynamical relaxation: An examination of the technique. *Quart. J. Roy. Meteor. Soc. 103*, 225–245.

Deardorff, J. W. 1972. Parameterization of the planetary boundary layer for use in general circulation models. *Mon. Wea. Rev. 100*, 93–106.

Errico, R. M. 1990. An analysis of dynamic balance in a mesoscale model. *Mon. Wea. Rev. 118*, 558–572.

Errico, R. M. and Baumhefner, D. P. 1987. Predictability experiments using a high-resolution limited-area model. *Mon. Wea. Rev. 115*, 488–504.

Errico, R. M. and Vukićević, T. 1992. Sensitivity analysis using an adjoint of the PSU/NCAR mesoscale model. *Mon. Wea. Rev. 120*, 1644–1660.

Lacarra, J.-F. and Talagrand, O. 1988. Short-range evolution of small perturbations in a barotropic model. *Tellus 40A*, 81–95.

Vukićević, T. and Errico, R. M. 1990. The influence of artificial and physical factors upon predictability estimates using a complex limited-area model. *Mon. Weather Rev. 118*, 1460–1482.